Bioconjugate Chemistry

Article

pubs.acs.org/bc

^{68}Ga/DOTA- and ^{64}Cu/NOTA-Phthalocyanine Conjugates as Fluorescent/PET Bimodal Imaging Probes

Elena Ranyuk,[†] Réjean Lebel,[†,∥] Yves Bérubé-Lauzière,[‡,∥] Klaus Klarskov,[§] Roger Lecomte,[†,∥] Johan E. van Lier,*[,†,∥] and Brigitte Guérin[#,†,∥]

[∥]Centre d'imagerie moléculaire de Sherbrooke (CIMS), [†]Departments of Nuclear Medicine and Radiobiology and [§]Pharmacology, Faculty of Medicine and Health Sciences, Université de Sherbrooke; 3001 12th Avenue North, Sherbrooke, Québec, Canada J1H 5N4

[‡]Department of Electrical and Computer Engineering, Université de Sherbrooke, 2500 boulevard Université, Sherbrooke, Québec, Canada J1K 2R1

Supporting Information

ABSTRACT: In this paper, we describe the synthesis and characterization of a series of new bimodal probes combining water-soluble sulfonated zinc phthalocyanine (ZnPc) as a fluorescence imaging unit and either ^{68}Ga/1,4,7,10-tetraazocyclododecane-*N*,*N*′*N*″,*N*′″-tetraacetic acid (DOTA) or ^{64}Cu/1,4,7-triazacyclononane-1,4,7-triacetic acid (NOTA) for PET imaging. The two moieties were linked through aliphatic chains of different lengths to modulate amphiphilicity. Labeling of DOTA− or NOTA−ZnPc conjugates with ^{68}Ga ($t_{1/2}$ = 68 min) and ^{64}Cu ($t_{1/2}$ = 12.7 h) was performed at 100 °C for 15 min with >90% efficiency for all conjugates. *In vitro* plasma stability assays demonstrated high stability of the ^{64}Cu/NOTA-ZnPc conjugate, which remained intact over a 24 h time period, and reasonably high stability of the ^{68}Ga/DOTA-ZnPc conjugate, which released up to 7% of free ^{68}Ga over a 3 h period. Based on *in vitro* plasma stability results, we performed biodistribution studies on two ^{64}Cu-labeled derivatives, which allowed us to select a single candidate for preliminary *in vivo* experiments. Fluorescence and PET imaging confirmed the potential of these novel conjugates to act as bimodal probes.

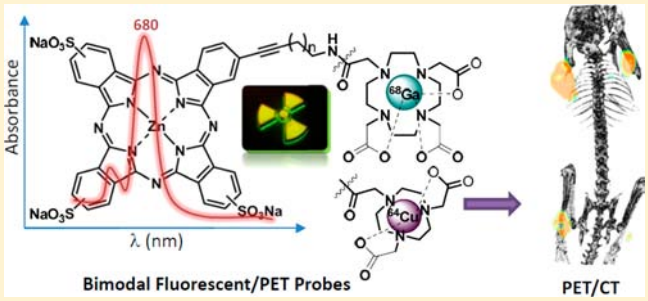

INTRODUCTION

A steadily increasing number of scientific papers and the rising interest at scientific meetings attest that there has been a surge in research on multimodal contrast agent development over the past few years.[1] Multimodal contrast agents can be visualized using different imaging techniques in parallel. No single molecular imaging modality is perfect and capable of providing all necessary information to answer a particular question.[2] For example, it is difficult to obtain quantitative information using fluorescence imaging (FI) alone, since it is limited by depth of light penetration and scatter of emitted light photons; magnetic resonance imaging (MRI) has high resolution and exquisite soft tissue contrast, yet it suffers from very low sensitivity; radionuclide-based imaging techniques are very sensitive and highly quantitative, but they have poor spatial resolution. Therefore, combining different molecular imaging modalities offers synergistic advantages over any single modality allowing high-resolution, high-sensitivity investigations of specific biological activities.[3]

Among prevailing imaging modalities used in biomedical research, optical imaging is currently the most widely used method.[3] Strengths of this technique include high sensitivity and direct detection of signals with simple optical devices, while the major disadvantage is poor light penetration through soft tissues and quantitation. Consequently, bimodal imaging probes that use optical imaging and positron emission tomography (PET) or MRI in tandem are attractive, as they take advantage of strengths of each imaging modality. For example, after lesion localization and surgery planning using PET or MRI, optical imaging may guide surgical procedure. Also, the combination of PET and FI can provide complementary information in small animal models where light penetration is less of an issue.

Water-soluble sulfonated metallo-phthalocyanines (MPc) are NIR fluorophores that possess high extinction coefficients, favorable quantum yields, and display extraordinarily high photostabilities.[4] These qualities make them particularly attractive for FI applications along with other important characteristics such as high water-solubility and reduced aggregation as compared to nonsubstituted Pc, as well as tumor-localizing properties and low toxicity. There are several examples in the literature where phthalocyanine fluorescence was used to study *in vivo* fluorescence kinetics and localization of Pc.[5,6] Several sulfonated metallo-phthalocyanine analogues

Received: May 24, 2013
Revised: July 26, 2013
Published: August 12, 2013

have been demonstrated to be preferentially retained in tumors[7−11] with the amphiphilic derivatives showing the highest tumor-to-nontumor ratios.[7,11] Furthermore, sulfonated Pc are effective photosensitizers (PS) for photodynamic therapy (PDT) of cancer to kill tumor cells *in vitro*[12−17] and cause tumor regression *in vivo*.[7,18−24] Several Pc-based PS have been investigated in preclinical and clinical trials and their potential therapeutic application in oncology was demonstrated.[25,26]

We recently reported the synthesis of ^{64}Cu-labeled sulfonated phthalocyanines ([^{64}Cu]CuPc) and their biodistribution using PET imaging.[11] The amphiphilic derivatives (disulfonated Pc and trisulfonated Pc bearing a lipophilic hexynyl chain) gave the highest tumor-to-background ratios. Unfortunately, CuPc are not fluorescent *in vivo* as opposed to ZnPc, so only a mixture of a fluorescent ZnPc and a corresponding radioactive [^{64}Cu]CuPc could be used as a bimodal imaging probe,[27] assuming that biodistribution of both ZnPc and CuPc is the same and does not depend on the central metal ion or *in vivo* concentration. Combining multimodal functionality in a single probe unit is not necessary for all applications, but there are advantages to this arrangement. A single multimodal probe helps ensure the same pharmacokinetics and localization of signal for each modality and eliminates additional stress on the body's blood clearance mechanisms that can accompany administration of multiple doses of agents.[1]

For this reason, we proceeded to prepare conjugates combining water-soluble fluorescent ZnPc and a multidentate chelating agent like DOTA (1,4,7,10-tetraazocyclododecane-*N*,*N*′*N*″,*N*′″-tetraacetic acid) or NOTA (1,4,7-triazacyclononane-1,4,7-triacetic acid). DOTA and NOTA derivatives are commercially available and their corresponding metal complexes are widely used as contrast agents for MRI as well as for PET and SPECT imaging. Besides, DOTA forms a stable complex with gallium(III) (formation constant, log K_{ML} = 21.33)[28] and therefore is widely used in preparation of ^{68}Ga-based PET probes as a chelating agent for ^{68}Ga(III), a radioisotope with high positron-emitting fraction (89% of its total decay) and half-life of 68 min. NOTA has been shown to form highly stable complexes with both Ga^{3+} and Cu^{2+} ions.[29,30]

In the current study, we report the synthesis of a series of new potential bimodal probes combining a water-soluble fluorescent sulfonated zinc phthalocyanine and a DOTA/NOTA moiety providing a stable chelating environment for $^{68}Ga^{3+}$ or $^{64}Cu^{2+}$ ions for PET-imaging. ZnPc and the polyazamacrocyclic moieties are linked together through an aliphatic chain of different lengths to modulate the amphiphilic character of the conjugates. Characterization, radiolabeling with ^{68}Ga and ^{64}Cu of the DOTA/NOTA-Pc conjugates, and *in vitro* stability of the resulting fluorescent/PET probes are presented. An imaging experiment with the most promising candidate is also described to confirm its potential as a bimodal probe for fluorescence and PET imaging.

EXPERIMENTAL SECTION

General Methods. Unless otherwise stated, all reactions were carried out under argon atmosphere. All chemicals and solvents were used as supplied without further purification. ^{1}H and ^{13}C NMR spectra were recorded on a 60/300 MHz spectrometer in $CDCl_3$ with the chemical shifts reported as δ in ppm and coupling constants expressed in Hz. The following abbreviations were used to describe spin multiplicity: s = singlet, d = doublet, t = triplet, q = quintet, dd = doublet of doublets, m = multiplet. Mass spectra were acquired in positive linear ion mode using a MALDI-TOF spectrometer (TofSpec 2E, Micromass/Waters). Samples were diluted with a saturated solution of α-cyano-4-hydroxycinnamic acid, prepared in 50% (v/v) aqueous acetonitrile containing 0.1% trifluoroacetic acid (TFA). Visible absorption spectra were recorded in 1 cm quartz cells. Analytical reverse phase HPLC was performed on a C18 semipreparative reverse phase column (10 × 250 mm, 5 μm) at a flow rate of 2 mL/min using a linear gradient of 0% to 100% MeOH in phosphate buffer (10 mM, pH 5.0) over 40 min. Purification of the target conjugates was performed on the same system. The identity of all new compounds was confirmed by MALDI-TOF and MALDI-TOF/TOF mass-spectrometry for HRMS, UV−vis spectroscopy, as well as by ^{1}H, ^{13}C NMR, and HRMS for the *N*-Boc-oct-7-yne. Due to aggregation and the presence of various regioisomers, the ^{1}H NMR signals of compounds **5**−**13** were not sufficiently resolved even at relatively low concentrations to obtain any accurate data. For these reasons, ^{1}H and ^{13}C NMR data are not reported for phthalocyanine derivatives **2**−**13**. Phthalocyanine derivatives can only be analyzed by MALDI-TOF. In reflector mode, a mass accuracy below 60 ppm can be readily obtained with the instrument. Copper-64 ($t_{1/2}$ = 12.7 h) was produced on a 19 MeV cyclotron by proton bombardment of an enriched Ni-64 plated rhodium disk (22 mm diameter, 1 mm thickness).[31] The target material was dissolved in HCl to give [^{64}Cu]$CuCl_2$ and converted to [^{64}Cu]$Cu(OAc)_2$ by dissolution in 0.1 M ammonium acetate buffer (0.1 mL), pH 5.5. The ^{68}Ga(III) was eluted from the ^{68}Ge/^{68}Ga generator (^{68}Ge $t_{1/2}$ = 270.8 days) using ∼6−7 mL of a solution of 0.1 N hydrochloric acid (HCl). Then, radioactive material was concentrated and purified on a cation exchange resin following a literature method.[30,32] The ^{68}Ga(III) was eluted from the resin with 800 μL of an 97.6% acetone/0.05 N HCl mixture (pH 2.3). Then, 500 μL of HEPES buffer (1 M, pH 4.0) was added and the resulting solution of ^{68}Ga(III) was used immediately for radiolabeling of DOTA-ZnPc conjugates. Radio thin-layer chromatography (TLC) was performed on an Instant Imager scanner (Bioscan, DC, U.S.A.) using C18 TLC plates and 15% methanol in sodium citrate buffer (1 M, pH 5.5) as a developing solvent. Fluorescence spectra were acquired in methanol in an Infinite M1000 PRO microplate reader.

General Procedure for Boc-Protection of Acetylenic Amines. To a stirred solution of an acetylenic amine (3 mmol) in a THF:H_2O (1:1, 20 mL) mixture were sequentially added Na_2CO_3 (3 equiv, 0.95 g, 9 mmol) and Boc_2O (1.5 equiv, 0.98 g, 4.5 mmol). After 3 h, the reaction mixture was extracted with EtOAc (2×). The combined organic layers were then dried ($MgSO_4$), filtered, and concentrated under reduced pressure. The residue was purified on silica gel utilizing 10% EtOAc/hexane.

N-Boc-3-Butynylamine. Prepared according to the general procedure from 3-butynylamine. The product was obtained as a colorless oil (0.35 g, 70% yield). The characterization data for *N*-Boc-3-butynylamine were in agreement with previously reported data.[33]

N-Boc-5-Hexynylamine. Prepared according to the general procedure from 5-hexynylamine. The product was obtained as a colorless oil (0.38 g, 65% yield). The characterization data for *N*-Boc-5-hexynylamine were in agreement with previously reported data.[34]

N-Boc-7-Octynylamine. Prepared according to the general procedure from 7-octynylamine. The product was obtained as a colorless oil (0.43 g, 64% yield): ^{1}H NMR (300 MHz, $CDCl_3$) δ 1.32−1.59 (m, 17H), 1.97 (t, 2H, J = 3.0 Hz), 2.22 (td, 2H, J = 6.0, 3.0 Hz), 3.14 (m, 2H), 4.54 (br. s, 1H); ^{13}C NMR (75.5 MHz, $CDCl_3$) δ 18.3, 26.3, 28.4, 30.0, 40.7, 68.2, 79.2, 84.6, 156.0; MALDI-TOF HRMS calcd for $C_8H_{16}N$ [(M+H)$^+$ - BOC] 126.1283, found: 126.1209 (Δm 59 ppm).

General Procedure for Sonogashira Cross-Coupling of ZnPc 1 and a Boc-Protected Acetylenic Amine. $Pd(OAc)_2$ (1.1 mg, 50 mol.%), (*o*-tolyl)$_3$P (4.5 mg, 150 mol.%), phthalocyanine **1** (10 mg, 0.01 mmol), and a Boc-protected acetylenic amine (0.1 mmol, 10-fold excess) were assembled in a round-bottomed flask sealed with a septum. The reaction flask was evacuated and purged with argon three times. Subsequently, 1 μL of degassed DMF was added under argon, followed by addition of DIPEA (∼30 μL, ∼15 equiv) degassed beforehand by gentle bubbling Ar through it for 30 min. The reaction mixture was stirred at 70 °C for 1−2 h. Thereafter, solvent was evaporated under reduced pressure to 50−100 μL. Phthalocyanines were precipitated using ethyl acetate, washed subsequently with large amounts of ethyl acetate and methanol, and dried *in vacuo* to give the desired crude product ZnPc-C_n-NHBoc (n = 1, 3, 5), **2**−**4**. This product was used for the next step without further purification. The identity of the products was confirmed by MALDI-TOF for their unprotected analogues and UV−vis spectrometry.

*Zinc (N-Boc-4-aminobut-1-ynyl)phthalocyanine Trisulfonate, Sodium Salt (ZnPc-C_4−NHBoc, **2**).* Prepared according to the general procedure from **1** and N-Boc-3-butynylamine. The product was obtained as a dark-blue powder (9.2 mg, 88%): MALDI-TOF MS (m/z): [(M+H)$^+$] calcd for $C_{36}H_{22}N_9O_9S_3Zn$ 886.2, found 886.3, [(2M+H)$^+$] calcd for $C_{72}H_{43}N_{18}O_{18}S_6Zn_2$ 1771.4, found 1769.7; UV−vis: λ_{max} (DMF): 680, 614 (sh), 353; HPLC (675 nm): four close peaks, t_R 30.3−32.3 min.

*Zinc (N-Boc-6-aminohex-1-ynyl)phthalocyanine Trisulfonate, Sodium Salt (ZnPc-C_6−NHBoc, **3**).* Prepared according to the general procedure from **1** and N-Boc-5-hexynylamine. The product was obtained as a dark-blue powder (9.7 mg, 90%): MALDI-TOF MS (m/z): [(M+H)$^+$] calcd for $C_{38}H_{26}N_9O_9S_3Zn$ 914.3, found 914.4, [(2M+H)$^+$] calcd for $C_{76}H_{51}N_{18}O_{18}S_6Zn_2$ 1827.6, found 1826.0; UV−vis: λ_{max} (DMF): 680, 614 (sh), 356; HPLC (675 nm): four close peaks, t_R 31.0−33.2 min.

*Zinc (N-Boc-8-aminooct-1-ynyl)phthalocyanine Trisulfonate, Sodium Salt (ZnPc-C_8−NHBoc, **4**).* Prepared according to the general procedure from **1** and N-Boc-7-octynylamine. The product was obtained as a dark-blue powder (10.0 mg, 90%): MALDI-TOF MS (m/z): [(M+H)$^+$] calcd for $C_{40}H_{30}N_9O_9S_3Zn$ 942.3, found 942.9, [(2M+H)$^+$] calcd for $C_{80}H_{59}N_{18}O_{18}S_6Z_2$ 1885.6, found 1883.5; UV−vis: λ_{max} (DMF): 680, 613 (sh), 355; HPLC (675 nm): four close peaks, t_R 29.8−33.8 min.

General Procedure for Boc-Deprotection of ZnPc-C_n-NHBoc (n = 1, 3, 5), 2−4. To a suspension of the carbamate ZnPc-C_n-NHBoc (n = 1, 3, 5), **2**−**4** (0.007 mmol), in CH_2Cl_2 (5 mL) at room temperature was added trifluoroacetic acid (2 mL). Immediately the product precipitated as a dark-green solid, and the reaction was stirred 30 min more to ensure completion of the reaction. As confirmed by RP-HPLC, the product was isolated by filtration, washed subsequently with large amounts of ethyl acetate and methanol and dried *in vacuo* to give the desired product ZnPc-C_n-$NH_3^+OTf^-$ (n = 1, 3, 5), **5**−**7**, without the need of further purification.

*Zinc (4-Aminobut-1-ynyl)phthalocyanine Trisulfonate, Ammonium Salt (ZnPc-C_4−NH_3^+OTf, **5**).* Prepared according to the general procedure from ZnPc-C_4−NHBoc, **2**. The product was obtained as a dark-green solid (7.1 mg, quant.): MALDI-TOF MS (m/z): [(M+H)$^+$] calcd for $C_{36}H_{22}N_9O_9S_3Zn$ 886.2, found 886.3, [(2M+H)$^+$] calcd for $C_{72}H_{43}N_{18}O_{18}S_6Zn_2$ 1771.4, found 1769.7; MALDI-TOF HRMS calcd for $C_{36}H_{22}N_9O_9S_3Zn$ [(M+H)$^+$] 883.9994, found: 883.9924 (Δm 8 ppm); UV−vis: λ_{max} (DMF): 680, 613 (sh), 348; HPLC (675 nm): four close peaks, t_R 19.0−25.2 min.

*Zinc (6-Aminohex-1-ynyl)phthalocyanine Trisulfonate, Ammonium Salt (ZnPc-C_6−NH_3^+OTf, **6**).* Prepared according to the general procedure from ZnPc-C_6−NHBoc, **3**. The product was obtained as a dark-green solid (7.4 mg, quant.): MALDI-TOF MS (m/z): [(M+H)$^+$] calcd for $C_{38}H_{26}N_9O_9S_3Zn$ 914.3, found 914.4, [(2M+H)$^+$] calcd for $C_{76}H_{51}N_{18}O_{18}S_6Zn_2$ 1827.6, found 1826.0; MALDI-TOF HRMS calcd for $C_{38}H_{26}N_9O_9S_3Zn$ [(M+H)$^+$] 912.0307, found: 912.0186 (Δm 13 ppm); UV−vis: λ_{max} (DMF): 680, 613 (sh), 348; HPLC (675 nm): three close peaks, t_R 20.9−24.8 min.

*Zinc (8-Aminooct-1-ynyl)phthalocyanine Trisulfonate, Ammonium Salt (ZnPc-C_8−NH_3^+OTf, **7**).* Prepared according to the general procedure from ZnPc-C_8−NHBoc, **4**. The product was obtained as a dark-green solid (7.5 mg, quant.): MALDI-TOF MS (m/z): [(M+H)$^+$] calcd for $C_{40}H_{30}N_9O_9S_3Zn$ 942.3, found 942.9, [(2M+H)$^+$] calcd for $C_{80}H_{59}N_{18}O_{18}S_6Z_2$ 1885.6, found 1883.5; MALDI-TOF HRMS calcd for $C_{40}H_{30}N_9O_9S_3Zn$ [(M+H)$^+$] 940.0620, found: 940.0494 (Δm 13 ppm); UV−vis: λ_{max} (DMF): 680, 614 (sh), 349; HPLC (675 nm): four close peaks, t_R 24.5−28.4 min.

General Procedure for the Synthesis of DOTA/NOTA-ZnPc Conjugates. To a solution of ZnPc-C_n-$NH_3^+OTf^-$ (n = 1, 3, 5), **5**−**7** (0.008 mmol), in a 5:1 mixture (1.2 mL) of DMF and Et_3N was added DOTA-NHS ester (3 equiv, 0.024 mmol, 18.2 mg) or NOTA-NHS ester (3 equiv, 0.024 mmol, 9.6 mg). If after 30 min of stirring, dissolution of Pc was not complete, deionized water was added in 100 μL portions. The reaction was stopped after MALDI-TOF analysis revealed complete disappearance of the starting amino-substituted Pc (12−24 h). When the reaction was incomplete, 2 equiv more of NHS-ester of DOTA (12.1 mg, 0.016 mmol) or NOTA (6.4 mg, 0.016 mmol) were added and the stirring continued until completion (6−12 h). After that the solvent was evaporated under reduced pressure to a final volume of 50−100 μL, Pc was precipitated using 1 N HCl, filtrated off, and washed subsequently with large amounts of water and MeOH to give the desired crude conjugate DOTA/NOTA-C_n-ZnPc (n = 1, 3, 5), **8**−**13** in acidic form. The solid was dissolved in a minimum volume of 1 M NaOH, diluted with deionized water, and purified on preconditioned (methanol followed by water) Sep Pack C18 cartridge eluted with water and methanol−water (1:4, v/v). The blue-green methanol−water fraction was evaporated *in vacuo* and the dark-blue residue was redissolved in a minimum volume of water and freeze-dried to yield the pure product. The analytical sample was further purified by semipreparative RP-HPLC using linear gradient of MeOH in phosphate buffer (10 mM, pH 5) over 40 min.

Zinc 4-[(4,7,10-Tri(carboxymethyl)-1,4,7,10-tetraazacyclodec-1-yl)acetamido]but-1-ynyl) Phthalocyanine Trisulfonate,

*Sodium Salt (DOTA-C_4–ZnPc, **8**).* Prepared according to the general procedure from ZnPc-C_4–$NH_3^+OTf^-$, **5**, and DOTA-NHS ester. The product was obtained as a blue-green solid (7.2 mg, 65%): MALDI-TOF MS (*m*/*z*): [(M+H)$^+$] calcd for $C_{52}H_{48}N_{13}O_{16}S_3Zn$ 1272.6, found 1273.2, [(M-CO_2+H)$^+$] calcd for $C_{51}H_{48}N_{13}O_{14}S_3Zn$ 1227.6, found 1228.1, [(2M+H)$^+$] calcd for $C_{104}H_{95}N_{26}O_{32}S_6Zn_2$ 2544.2, found 2544.0; MALDI-TOF HRMS calcd for $C_{52}H_{48}N_{13}O_{16}S_3Zn$ [(M+H)$^+$] 1270.1796, found: 1270.2090 (Δm 23 ppm); UV–vis λ_{max} (DMF): 680, 614 (sh), 348; HPLC (675 nm): two close broad peaks, t_R 22.1–23.9 min.

*Zinc 6-[(4,7,10-Tri(carboxymethyl)-1,4,7,10-tetraazacyclododec-1-yl)acetamido]hex-1-ynyl) Phthalocyanine Trisulfonate, Sodium Salt (DOTA-C_6–ZnPc, **9**).* Prepared according to the general procedure from ZnPc-C_6–$NH_3^+OTf^-$, **6**, and DOTA-NHS ester. The product was obtained as a blue-green solid (8.0 mg, 70%): [(M+H)$^+$] calcd for $C_{54}H_{52}N_{13}O_{16}S_3Zn$ 1300.7, found 1300.9, [(M-CH_2COOH+H)$^+$] calcd for $C_{52}H_{50}N_{13}O_{14}S_3Zn$ 1242.6, found 1243.2; UV–vis λ_{max} (DMF): 681, 614 (sh), 351; HPLC (675 nm): four close peaks, t_R 26.1–28.6 min.

*Zinc 8-[(4,7,10-Tri(carboxymethyl)-1,4,7,10-tetraazacyclododec-1-yl)acetamido]oct-1-ynyl) Phthalocyanine Trisulfonate, Sodium Salt (DOTA-C_8–ZnPc, **10**).* Prepared according to the general procedure from ZnPc-C_8–$NH_3^+OTf^-$, **7**, and DOTA-NHS ester. The product was obtained as a blue-green solid (8.5 mg, 73%): MALDI-TOF MS (*m*/*z*): [(M+H)$^+$] calcd for $C_{56}H_{56}N_{13}O_{16}S_3Zn$ 1328.7, found 1329.1, [(M-CO_2+H)$^+$] calcd for $C_{51}H_{48}N_{13}O_{14}S_3Zn$ 1284.7, found 1284.3, [(2M+H)$^+$] calcd for $C_{55}H_{56}N_{13}O_{14}S_3Zn$ 2656.4, found 2654.9; MALDI-TOF HRMS calcd for $C_{56}H_{56}N_{13}O_{16}S_3Zn$ [(M+H)$^+$] 1326.2422, found: 1326,1923 (Δm 38 ppm); UV–vis λ_{max} (DMF): 682, 617 (sh), 354; HPLC (675 nm): six close peaks, t_R 28.2–31.2 min.

*Zinc 4-[(4,7-Di(carboxymethyl)-1,4,7-triazacyclononan-1-yl)acetamido]but-1-ynyl) Phthalocyanine Trisulfonate, Sodium Salt (NOTA-C_4–ZnPc, **11**).* Prepared according to the general procedure from ZnPc-C_4–$NH_3^+OTf^-$, **5**, and NOTA-NHS ester. The product was obtained as a blue-green solid (7.2 mg, 70%): MALDI-TOF MS (*m*/*z*): [(M+H)$^+$] calcd for $C_{48}H_{41}N_{12}O_{14}S_3Zn$ 1171.5, found 1171.9, [(M-CO_2+H)$^+$] calcd for $C_{47}H_{41}N_{12}O_{12}S_3Zn$ 1127.5, found 1127.9; MALDI-TOF HRMS calcd for $C_{48}H_{41}N_{12}O_{14}S_3Zn$ [(M+H)$^+$] 1169.1319, found: 1169, 1992 (Δm 58 ppm);UV–vis λ_{max} (DMF): 681, 614 (sh), 353; HPLC (675 nm): three broad close peaks, t_R 24.6–27.0 min.

*6-[(4,7-Di(carboxymethyl)-1,4,7-triazacyclononan-1-yl)-acetamido]hex-1-ynyl) Phthalocyanine Trisulfonate, Sodium Salt (NOTA-C_6–ZnPc, **12**).* Prepared according to the general procedure from ZnPc-C_6–$NH_3^+OTf^-$, **6**, and NOTA-NHS ester. The product was obtained as a blue-green solid (6.6 mg, 64%): MALDI-TOF MS (*m*/*z*): [(M+H)$^+$] calcd for $C_{50}H_{45}N_{12}O_{14}S_3Zn$ 1199.6, found 1200.0, [(M-CH_2COOH+H)$^+$] calcd for $C_{48}H_{43}N_{12}O_{12}S_3Zn$ 1141.5, found 1142.2; MALDI-TOF HRMS calcd for $C_{50}H_{45}N_{12}O_{14}S_3Zn$ [(M+H)$^+$] 1197.1632, found: 1197.2046 (Δm 35 ppm);UV–vis λ_{max} (DMF): 682, 615 (sh), 352; HPLC (675 nm): four close broad peaks, t_R 26.5–28.7 min.

*8-[(4,7-Di(carboxymethyl)-1,4,7-triazacyclononan-1-yl)-acetamido]oct-1-ynyl) Phthalocyanine Trisulfonate, Sodium Salt (NOTA-C_8–ZnPc, **13**).* Prepared according to the general procedure from ZnPc-C_8–$NH_3^+OTf^-$, **7**, and NOTA-NHS ester. The product was obtained as a blue-green solid (7.1 mg, 67%): MALDI-TOF MS (*m*/*z*): [(M+H)$^+$] calcd for $C_{52}H_{49}N_{12}O_{14}S_3Zn$ 1227.6, found 1127.8, [(M-CH_2COOH+H)$^+$] calcd for $C_{50}H_{47}N_{12}O_{12}S_3Zn$ 1169.6, found 1170.7; MALDI-TOF HRMS calcd for $C_{52}H_{49}N_{12}O_{14}S_3Zn$ [(M+H)$^+$] 1225.1945, found: 1225.2158 (Δm 17 ppm);UV–vis λ_{max} (DMF): 681, 615 (sh), 352; HPLC (675 nm): three close broad peaks, t_R 28.6–31.6 min.

General Procedure for the ^{68}Ga-Radiolabeling. A solution of DOTA-ZnPc conjugate **8**–**10** (10 μL, 430 μM) in deionized water was added to ~500 μL of HEPES buffer/acetone containing ~165 MBq (~4.5 mCi) of ^{68}Ga(III). The reaction vial was heated at 95–100 °C for 15 min. Reaction progress was followed by radio-TLC to confirm completion of the radiolabeling. The resulting blue solution was passed through a preconditioned (methanol followed by water) reversed-phase Sep-Pak C18 cartridge. The cartridge was washed with water (10 mL). Thereafter, the blue radioactive product was eluted with 2 mL of MeOH. The ^{68}Ga/DOTA-C_n-Pc fraction was collected, evaporated, and counted in a Capintec radioisotope calibrator (Capintec, Inc., NJ, USA) to determine the specific activity of the product. The solvent was evaporated to dryness to yield the ^{68}Ga/DOTA-C_n-Pc (**14**–**16**) as a blue solid (radiochemical purity >98%, as checked by radio-TLC) in ~60% decay-corrected yield.

Non-radiolabeled analogues Ga/DOTA-C_n-ZnPc (**14**–**16**) were prepared in a similar manner using $GaCl_3$.

*Compound Ga/DOTA-C_4–ZnPc, **14**.* MALDI-TOF MS (*m*/*z*): [(M+H)$^+$] calcd for $C_{52}H_{46}GaN_{13}O_{16}S_3Zn$ 1340.3, found 1340.6; UV–vis λ_{max} (DMF): 680, 614 (sh), 347.

*Compound Ga/DOTA-C_6–ZnPc, **15**.* MALDI-TOF MS (*m*/*z*): [(M+H)$^+$] calcd for $C_{54}H_{50}GaN_{13}O_{16}S_3Zn$ 1368.4, found 1368.6; UV–vis λ_{max} (DMF): 680, 614 (sh), 350.

*Compound Ga/DOTA-C_8–ZnPc, **16**.* MALDI-TOF MS (*m*/*z*): [(M+H)$^+$] calcd for $C_{56}H_{54}GaN_{13}O_{16}S_3Zn$ 1396.4, found 1396.3; UV–vis λ_{max} (DMF): 681, 614 (sh), 353.

General Procedure for the ^{64}Cu-Radiolabeling. A solution of NOTA-ZnPc conjugates **11**–**13** (20 μL, 800 μM) in deionized water was added to a solution of [^{64}Cu]Cu(OAc)$_2$ (~130 MBq; ~3.5 mCi) in 150–200 μL of ammonium acetate buffer (0.1 M, pH 5.5). The reaction mixture was heated at 95–100 °C for 15 min. Radio-TLC revealed product formation in decay-uncorrected yields ranging from 90% to 100%. The resulting blue solution was passed through a reversed-phase Sep-Pak C18 cartridge and the product was absorbed on the cartridge. The cartridge was then washed with water (3 × 10 mL); thereafter, the blue radioactive product was eluted with 2 mL of MeOH. The ^{64}Cu/NOTA-C_n-Pc fraction was collected, evaporated, and counted in a Capintec radioisotope calibrator (Capintec, Inc., NJ, USA) to determine the specific activity of the product. The solvent was evaporated to dryness to give ^{64}Cu/NOTA-C_n-Pc (**17**–**19**) as a blue solid (radiochemical purity >95%, as checked by radioactive TLC) in ~70% decay-uncorrected yield.

Non-radiolabeled analogues Cu/NOTA-C_n-ZnPc (**17**–**19**) were prepared in a similar manner using Cu(II) acetate.

*Compound Cu/NOTA-C_4–ZnPc, **17**.* MALDI-TOF MS (*m*/*z*): [(M+H)$^+$] calcd for $C_{48}H_{39}CuN_{12}O_{14}S_3Zn$ 1233.0, found 1233.2; UV–vis λ_{max} (DMF): 681, 614 (sh), 347.

*Compound Cu/NOTA-C_6–ZnPc, **18**.* MALDI-TOF MS (*m*/*z*): [(M+H)$^+$] calcd for $C_{50}H_{43}CuN_{12}O_{14}S_3Zn$ 1261.1, found 1261.1; UV–vis λ_{max} (DMF): 682, 616 (sh), 349.

dx.doi.org/10.1021/bc400257u | *Bioconjugate Chem.* 2013, 24, 1624–1633

*Compound Cu/NOTA-C_8–ZnPc, **19**.* MALDI-TOF MS (m/z): [$(M+H)^+$] calcd for $C_{52}H_{47}CuN_{12}O_{14}S_3Zn$ 1289.2, found 1289.5; UV–vis λ_{max} (DMF): 682, 616 (sh), 348.

***In Vitro* Plasma Stability Studies.** The purified radiolabeled [^{68}Ga]-**14**/[^{64}Cu]-**17** (111 MBq; 3 mCi) in 50 μL of water was mixed with 150–200 μL of mouse plasma (n = 3) and heated at 37 °C for a maximum period of 3 h for ^{68}Ga- and 24 h for ^{64}Cu-labeled analogue, respectively. Stability of radiolabeled compounds was analyzed by radio-TLC with free [^{68}Ga]$GaCl_3$/[^{64}Cu]$Cu(OAc)_2$ and purified radiolabeled conjugates used as standards. TLC was performed either on silica gel coated plastic sheets with methanol/0.1 M ammonium acetate pH 5.5 (1:1) as eluent, or on C-18 bonded reversed-phase TLC plates with 0.1 M sodium citrate at pH 5, and ^{64}Cu was detected by an Instant Imager system.

Animal Models and Biodistributions. For imaging and biodistribution studies, 3 nude mice were implanted with MC7-L1 tumors (above hips and shoulders) by subcutaneous injections of 10^7 cells. Two EMT-6 tumors were similarly implanted using 2.5×10^5 cells. Timing of these injections was adjusted to compensate for the difference in the rate of growth of both tumor types. For 3 h postinjection biodistribution studies, 7 Balb/C mice were prepared as described above. To determine the *in vivo* distribution of the bimodal probes, mice were injected with 1.7 ± 0.3 MBq (100 μL) of either ZnPc-C_4–NOTA ^{64}Cu or ZnPc-C_8–NOTA-^{64}Cu via the caudal vein. The animals were sacrificed with CO_2 at 3 or 25 h postinjection [p.i.]. Organs of interest were collected, weighed, and counted in a gamma counter. The results are expressed as percentage of the injected dose per gram of tissue [%ID/g].

Imaging Experiments. Imaging studies were performed on 3 nude mice. For each imaging session, mice were anesthetized (2.5% induction, 1.5% isoflurane in medical O_2). In the initial session, a cannula was inserted in a caudal vein of the mice to inject the bimodal probe (20 ± 5 MBq, 54 ± 8 pmol/g). Each animal was then placed prone on a custom-made multimodal bed and imaged using the following sequence: FI (−1 min), Injection, FI (0–10 min), CT (10–15 min), PET (22–38 min), FI (45 min), PET (52–68 min), MRI (80–90 min), before being awakened. Next, imaging sequences (anesthesia, PET, and FI) were performed at 3, 6, 11, and 25 h. Each time, the animal was repositioned on the multimodal bed. The animals were euthanized after the last imaging session, reimaged in FI, and their organs extracted for FI and biodistribution studies.

Fluorescence Imaging. FI acquisitions were performed on the Quidd Optical Scanner (Quidd, Val de Reuil, France) using the following filters: Excitation [655/40 nm bandpass filter (Semrock, Rochester, NY, USA)] and emission [715/40 nm bandpass filter (Semrock, Rochester, NY, USA) nm +695 nm long-pass Schott glass absorptive filter (Edmund Optics, Barrington, NJ, USA)]. Thirty seconds acquisitions were performed at 50% lighting intensity. After euthanasia, animals were imaged prone on a flat surface using the same conditions as above. Organs were also imaged similarly.

PET and CT Imaging. PET and CT scans were performed using a LabPET8 (Gamma Medica-IDEAS Inc., Sherbrooke, Quebec, Canada) small-animal scanner with a field of view of 7.5 cm. Fifteen minute static acquisitions were performed at postinjection time T = [0.5 h; 1 h; 3 h; 6 h; 11 h], and a 30 min acquisition was performed at T = [25 h]. This single larger time frame was used to compensate for ^{64}Cu decay at this advanced time point. Reconstruction was performed using a 60 mm FOV (120 × 120 voxels matrix) with axial thickness of 0.59 mm.

MRI Imaging. T_2-weighted images were acquired at 1.2 h postinjection using a Varian 7T small animal scanner (Varian Inc. Palo Alto, CA, USA) and a 60 mm volume coil using the following parameters: TR: 6 s, TE: 12 ms, echoes: 8, averages: 4, data matrix: 128 × 128, field of view: 35 mm × 35 mm, number of slices: 60, slice thickness: 1.5 mm. Note that the probe does not generate contrast in MRI, which was performed to acquire anatomical information.

Image Registration and Analysis. Images were analyzed using in-house Matlab modules and functions. Fluorescence images (Figure 2D) were corrected for background when possible (T = 10 and 45 min – during which the animal was not moved) using the preinjection image. The PET surface image (Figure 1F) was calculated from the top non null voxels (5 mm, 10 voxels). Co-registration of PET and MR imaging was performed manually, and is presented here for display only (no analysis). MRI and PET images were interpolated for

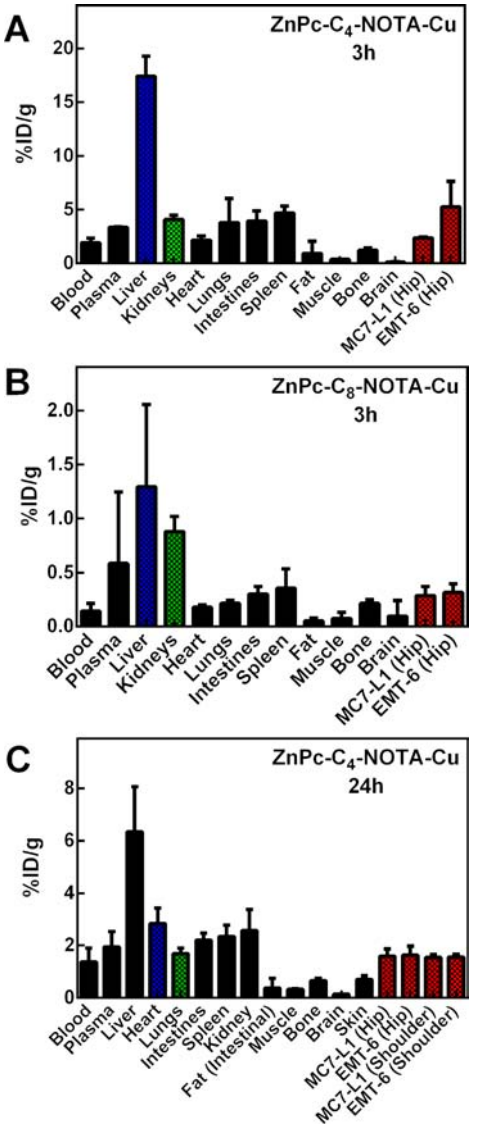

Figure 1. Biodistributions of ^{64}Cu/NOTA-C_4–ZnPc (A) and ^{64}Cu/NOTA-C_8–ZnPc (B) 3 h PI; Biodistribution of ^{64}Cu/NOTA-C_4–ZnPc (C) 25 h PI after the imaging experiment.

dx.doi.org/10.1021/bc400257u | *Bioconjugate Chem.* 2013, 24, 1624–1633

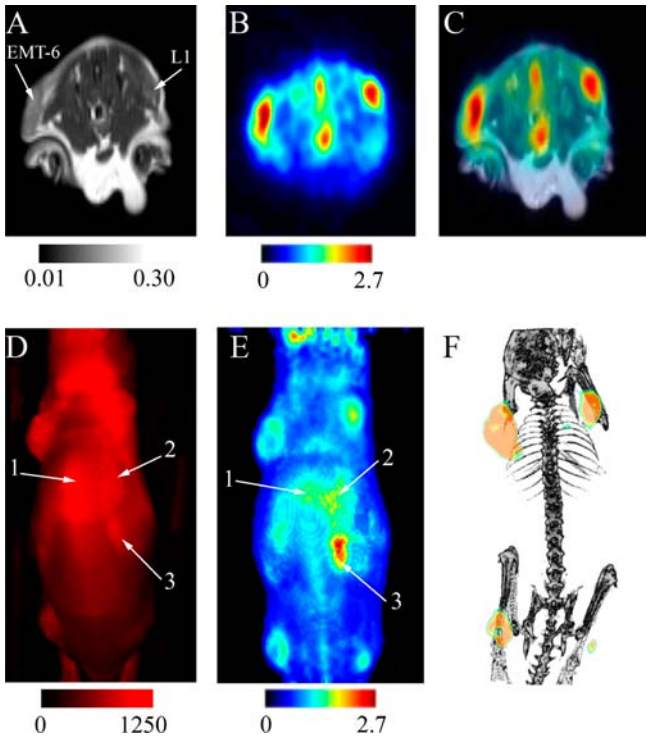

Figure 2. Imaging of ^{64}Cu/NOTA-C_4–ZnPc in tumor bearing nude mice. (A) MRI T_2-weighted anatomical maps support the location of tumors, which have a good contrast against surrounding tissues in PET 1 h postinjection (B). These PET images show the tumors on the hips of the animal. Two additional high region areas, the spine and the tip of the bladder, are also visible. (C) Image fusion of PET and MRI allows us to locate the tumors. (D) FI imaging 45 min postinjection yields information about the surface distribution of the probe. Note that this fluorescence image was corrected for background fluorescence by subtracting the preinjection image. Hence, the probe is completely responsible for the signal shown here. (E) The surface distribution of the probe can also be extracted from PET. Here, the activity in the first 5 mm is averaged and presented as a coronal view. Arrows 1–3 in (D) and (E) point at similar regions of high concentration/activity (not at specific organs) for comparison between these modalities. (F) Tumors were cropped and merged with the CT scan of this animal (3D rendering). These results are for a single mouse (out of three) and are representative.

display purpose. Time activity curves (TACs) were extracted from regions of interests drawn and analyzed in an in-house Matlab module. The PET/CT registration was performed in Amide.[35]

RESULTS AND DISCUSSION

Synthesis. Scheme 1 depicts the sequence of reactions used to prepare DOTA/NOTA-ZnPc conjugates. Mono-iodinated sulfophthalocyanine **1** was prepared according to a previously reported procedure.[36] Boc-protected derivatives of 4-aminobut-1-yne, 6-aminohex-1-yne,[37] and 8-aminooct-1-yne[38] were prepared by reacting di-*tert*-butyl carbonate with a free amine in a 1:1 mixture of tetrahydrofuran and water in the presence of sodium bicarbonate. Phthalocyanine **1** was reacted under copper-free Sonogashira cross-coupling conditions[39,40] with three different Boc-protected acetylenic amines at 80 °C in the presence of palladium acetate [$Pd(OAc)_2$], tri(*o*-tolyl)-phosphine [$(o\text{-tolyl})_3P$], and *N*,*N*-diisopropylethylamine [DIPEA] in *N*,*N*-dimethylformamide (DMF). The reactions were complete within 1 h and the formation of the cross-coupled products ZnPc-C_n-NHBoc **2**–**4** along with the trace amounts of reduction product was confirmed by MALDI-TOF spectroscopy and analysis of RP-HPLC-profile of the reaction mixture at 675 nm (Table 1, entries 1–3). The target compounds were purified by ethyl acetate precipitation followed by washing with large amounts of ethyl acetate. Subsequent Boc-deprotection was performed in a 2:1 mixture of dichloromethane (CH_2Cl_2) and trifluoroacetic acid (TFA) at room temperature for 30 min. Corresponding unprotected products ZnPc-C_n-$NH_3^+OTf^-$ **5**–**7** precipitated from solution and were simply isolated by filtration followed by washing with ethyl acetate and methanol (Table 1, entries 4–6). The coupling reactions of **5**–**7** with 3–5-fold excess of mono-*N*-hydroxysuccinimide ester of DOTA or NOTA (DOTA-NHS ester and NOTA-NHS ester, respectively) were carried out in DMF in the presence of triethylamine (Et_3N). Completion of the reaction was followed by MALDI-TOF analysis; the coupling was normally complete within 12–36 h. The crude DOTA/NOTA-ZnPc conjugates **8**–**13** were isolated by acid precipitation followed by washing with large amounts of water and methanol (Table 1, entries 7–12). The desired products were subsequently purified on a C18 Sep-Pack cartridge eluted with water and methanol–water (1:4, v/v). Analytical samples were further purified by semipreparative HPLC using linear gradient of MeOH in phosphate buffer (10 mM, pH 5) over 40 min.

Radiochemistry. Radiolabeling of DOTA-ZnPc conjugates **8**–**10** with Ga-68 was performed in HEPES buffer (pH 4) at 95–100 °C for 15 min (Scheme 2). Radio-TLC confirmed completion of the radiolabeling. The radiolabeled product was purified on a C18 SepPak cartridge in H_2O/MeOH to yield ^{68}Ga/DOTA-C_n-ZnPc (**14**–**16**) in ~60% decay-corrected yield and radiochemical purity >98%, as checked by radio-TLC. Radiolabeling of the NOTA-ZnPc conjugates **11**–**13** was performed in 0.1 M ammonium acetate buffer (pH 5.5) using [^{64}Cu]Cu$(OAc)_2$. ^{64}Cu-incorporation was followed by radio-TLC and shown to be >90% within 15 min of heating at 95–100 °C. The radiolabeled products were purified on C18 SepPack cartridges in H_2O/MeOH, to yield the corresponding ^{64}Cu/NOTA-C_n-ZnPc (**17**–**19**) in ~70% non-decay-corrected yields and >95% radiochemical purities (Scheme 3). The specific activities measured were ~38 TBq/mmol for ^{68}Ga/DOTA-C_n-ZnPc (**14**–**16**), and 7 to 8 TBq/mmol for ^{64}Cu/NOTA-C_n-Pc (**17**–**19**). The specific activities of the ^{68}Ga/DOTA-C_n-ZnPc were slightly higher than that of the ^{64}Cu/NOTA-C_n-Pc when calculated on a molar basis. The observed variations in specific activity can be explained by the fact that different amounts of DOTA- and NOTA-C_n-ZnPc conjugates were used for the labeling, and the quantity of radioactivity varied in each case. Nonradioactive Cu(II) and Ga(III) complexes of the same conjugates were prepared in a similar manner using cold $GaCl_3$ or $Cu(OAc)_2$ and characterized by standard spectroscopic analyses.

Fluorescence Spectra of Cu/NOTA-C_4–ZnPc. The impact of NOTA addition and ^{64}Cu chelation was assessed. For this, the *in vivo* imaging candidate was compared to $ZnPcS_3C_6$. Spectra for $ZnPcS_3C_6$, NOTA-C_4–ZnPc, and Cu/NOTA-C_4–ZnPc were acquired and a minimal redshift was detected for last two compounds; see Supporting Information. Therefore, this shift is not expected to impact FOI experiments and fluorescence properties of sulfonated ZnPc are not affected by conjugation to another chelated metal.

dx.doi.org/10.1021/bc400257u | *Bioconjugate Chem.* 2013, 24, 1624–1633

Scheme 1. Synthesis of the DOTA/NOTA-ZnPc Conjugates

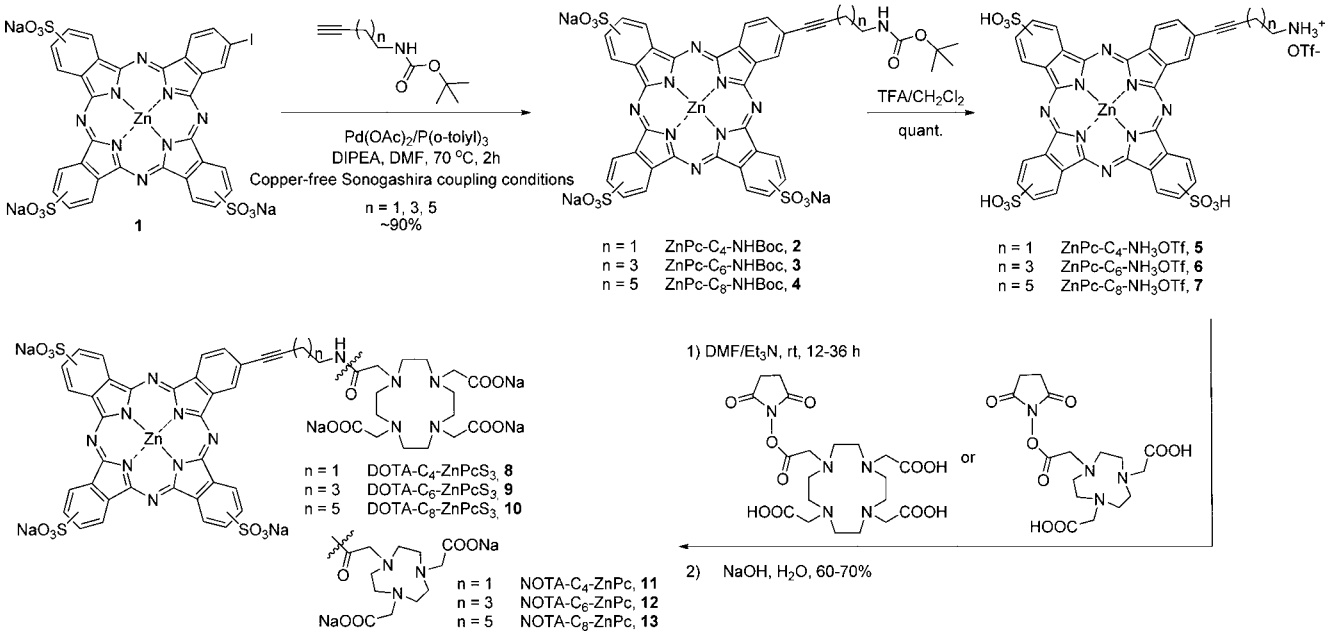

Table 1. Analytical Data for DOTA- and NOTA-Phthalocyanine Conjugates

		[M+H]$^+$		UV–vis,	RP-HPLC	yield
entry	product[a]	calcd[b]	found[b]	λ_{max}, nm (DMF)	t_R, min	%
1	ZnPc-C_4-DOTA, **8**	1272.6 1227.6[e] 2544.2[d]	1273.2 1228.1[e] 2544.0[d]	348, 614 (sh), 680	22.1–23.9	65
2	ZnPc-C_6-DOTA, **9**	1300.7 1242.6[f]	1300.9 1243.2[f]	351, 614 (sh), 681	26.1–28.6	70
3	ZnPc-C_8-DOTA, **10**	1328.7 1284.7[e] 2656.4[d]	1329.1 1284.3[e] 2654.9[d]	354, 617 (sh), 682	28.2–31.2	73
4	ZnPc-C_4–NOTA, **11**	1171.5 1127.5[e]	1171.9 1127.9[e]	353, 614 (sh), 681	24.6–27.0	70
5	ZnPc-C_6–NOTA, **12**	1199.6 1141.5[f]	1200.0 1142.2[f]	352, 615 (sh), 682	26.5–28.7	64
6	ZnPc-C_8–NOTA, **13**	1227.6 1169.6[f]	1227.8 1170.7[f]	352, 615 (sh), 681	28.6–31.6	67

[a]It is to be noted that **1** was obtained via statistical condensation and consequently is composed of mixture of positional isomers. [b]Average mass values obtained by MALDI-TOF spectroscopy. [c]ZnPc-C_n-NHBoc, **2**–**4**, were characterized in unprotected form as corresponding ZnPc-C_n-$NH_3^+OTf^-$, **5**–**7**. [d]Mass value is given for $[2M+H]^+$ adduct. [e]Mass value is given for $[M-CO_2+H]^+$. [f]Mass value is given for $[M-CH_2COOH+H]^+$

***In Vitro* Plasma Stability.** The stability *in vitro* of two radiolabeled conjugates, ^{68}Ga/DOTA-C_4–ZnPc **14** and ^{64}Cu/NOTA-C_4–ZnPc **17**, was studied in mouse plasma at 37 °C for a period of 3 h (^{68}Ga-analogue) and 24 h (^{64}Cu-labeled analogue). Radio-TLC on C18 performed directly on plasma samples without precipitating plasma proteins was used to determine ^{64}Cu metabolites and free ^{64}Cu(II). Free [^{68}Ga]-$GaCl_3$/[^{64}Cu]$Cu(OAc)_2$ and purified radiolabeled conjugates were used as standards. The radio-TLC analysis showed no degradation of the ^{64}Cu/NOTA-C_4–ZnPc **17** even after 24 h incubation in mouse plasma. Incubating ^{68}Ga/DOTA-C_4–ZnPc **14** in plasma, small amounts (~2%) of free ^{68}Ga(III) were detected after 15 min steadily increasing up to ~7% after 3 h.

Biodistribution of ^{64}Cu/NOTA-C_4–ZnPc and ^{64}Cu/NOTA-C_8–ZnPc. Given the plasma stability results, the ^{64}Cu/NOTA labeled compounds were selected for biodistribution assays. Note that none of these compounds possess targeting capabilities, therefore specific accumulation in any tissue is not expected. Since these molecules are relatively small (<5 kDa), they would only marginally benefit from the enhanced perfusion and retention effect, present in tumors. To minimize the number of animals needed, and to verify that the biodistribution profile of the bimodal probes can be affected by the spacer length between the chelator and the Pc, we compared ^{64}Cu/NOTA-C_4-Pc (n = 3) and ^{64}Cu/NOTA-C_8-Pc (n = 4). The results of these biodistribution studies are presented in Figure 1A,B. A ~10-fold larger retention was observed for ^{64}Cu/NOTA-C_4-Pc in most organs (note the scaling difference), which suggests that imaging experiments using this bimodal probe would likely result in better fluorescence and PET signal. Both profiles are similar in relative terms (e.g., organ/blood ratios), with one exception: ^{64}Cu/NOTA-C_8-Pc is relatively more present in the kidney (kidney/blood ratio of 2.1 and 6.1 for C_4 and C_8 compounds, respectively), suggesting that its larger clearance rate is due to renal excretion. The amplitude of this difference was surprising since the linker change is minimal. However, identifying the molecular determinants of this behavior is outside the scope of the current study.

Usually one would choose the molecule that is eliminated most quickly to provide a larger specific/nonspecific contrast during molecular imaging. However, our molecules lack specificity, and our objective here is to demonstrate that our probes can be used for multimodal imaging. Therefore, we selected ^{64}Cu/NOTA-C_4-Pc for its longer biological half-life to perform a preliminary multimodal imaging experiment.

Multimodal Imaging of ^{64}Cu/NOTA-C_4–ZnPc. We performed PET, CT, FI, and MRI of nude mice (n = 3), and assessed the potential of ^{64}Cu/NOTA-C_4–ZnPc as a bimodal imaging probe. Images for each modality are presented in

dx.doi.org/10.1021/bc400257u | *Bioconjugate Chem.* 2013, 24, 1624–1633

Scheme 2. Radiolabeling of DOTA−ZnPc Conjugates 8−10 with ^{68}Ga

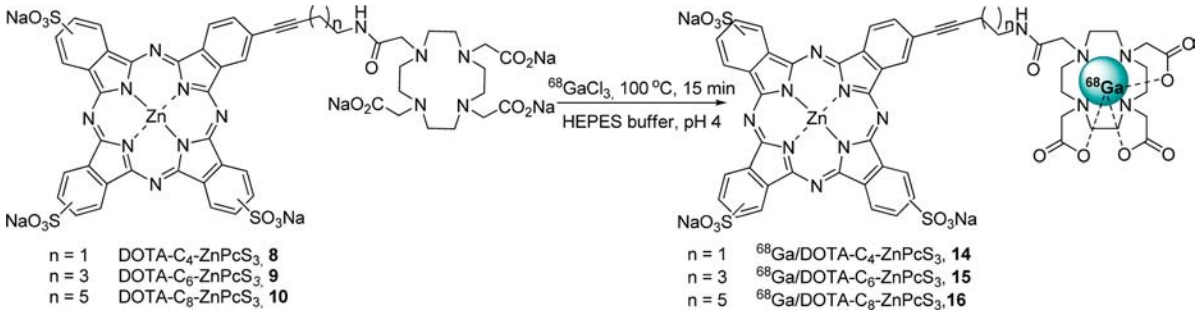

Scheme 3. Radiolabeling of NOTA−ZnPc Conjugates 11−13 with ^{64}Cu

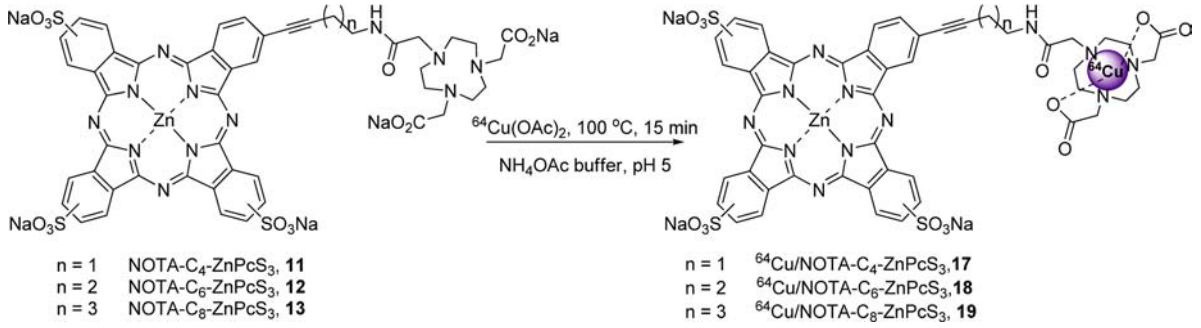

Figure 2. MRI (Figure 2A) and PET (Figure 2B, 1 h postinjection) acquisitions can be easily superposed (Figure 2C), and the anatomical information provided by MRI allows for the confirmation of the source of PET signal (e.g., in Figure 2A and B, the signal is located inside the tumors). Manual merging of PET and MRI as well as a 3D rendering of the cropped tumors in PET with the whole mouse CT scan are presented in Figure 2C and F, respectively. The nature of ^{64}Cu/NOTA-C_4−ZnPc does not allow for the specific targeting of tumors, which is reflected in the overall distribution pattern of this probe (Figure 1). This is also visible in the fluorescence images (Figure 2D, 45 min postinjection), reflecting the surface distribution of the probe (note that tumors are only slightly more intense than the rest of the animal). The complete FOI data set, as well as a representative PET data set (Supporting Information Figure 55) are also available.

In order to compare 3D PET with 2D FI, we calculated the average PET signal in the first 5 mm depth from the surface of the animal (Figure 2E). This calculation yielded the distribution of the probe on the animal's surface, as viewed from above, which is comparable to the FI. Note that the FI signal is mitigated by absorption, scattering, and view angle − hence a perfect correlation is not expected. However, Figure 2D and E is qualitatively similar and many features are visible in both images. The optical properties of our probes were found to be similar *in vitro* (data not shown). Overall, these data confirm that our probes can be used for multimodal imaging in PET and FI, justifying further development of analogs with improved target-specificity. Moreover, DOTA-ZnPc conjugates chelated with Gd(III) could provide a route to develop dual optical/MRI imaging probes.

CONCLUSION

We prepared a new series of water-soluble and stable bimodal fluorescent/PET probes, ^{68}Ga/DOTA− and ^{64}Cu/NOTA−phthalocyanine conjugates. DOTA-ZnPc conjugates were labeled with Ga-68 and NOTA-Pc conjugates with Cu-64, with radiolabeling efficiency higher than 90% for all the conjugates and excellent specific activity. Considering their high *in vitro* plasma stability, both ^{68}Ga/DOTA− and ^{64}Cu/NOTA−phthalocyanine conjugates were found to be promising candidates for dual fluorescence/PET imaging. Multimodal imaging of tumor bearing mice confirmed that our probes can be used for PET and FI.

ASSOCIATED CONTENT

Supporting Information

Copies of NMR spectra of N-Boc-7-octynlamine, HPLC traces of **1**−**4** and **8**−**13**, MALDI-TOF spectra of **5**−**13**, Ga/DOTA-C_n-ZnPc (**14**−**16**), and Cu/NOTA-C_n-ZnPc (**17**−**19**), UV−vis spectra of **2**−**13**, Ga/DOTA-C_n-ZnPc (**14**−**16**), and Cu/NOTA-C_n-ZnPc (**17**−**19**). Copies of MALDITOF HRMS spectra of **5**−**13** and N-Boc-7-octynylamine and Stability results for 68Ga/DOTA-C4ZnPc and 64Cu/NOTA-C4ZnPc. This material is available free of charge via the Internet at http://pubs.acs.org.

AUTHOR INFORMATION

Corresponding Authors

*E-mail: Johan.E.vanlier@USherbrooke.ca. Phone: (819) 564-5409. Fax: (819) 829-3238.

#E-mail: Brigitte.Guerin2@USherbrooke.ca. Phone: (819) 820-6868 ext. 15285. Fax: (819) 829-3238.

Notes

The authors declare no competing financial interest.

ACKNOWLEDGMENTS

B.G., Y.B.L., R.L., and J.E.v.L. are members of the *Fonds de la Recherche en Santé du Québec*-supported CRC Étienne-Le Bel of the *Centre Hospitalier Universitaire de Sherbrooke*, Sherbrooke, QC, Canada. This work was supported by an NSERC Strategic Projects Grant (Canada) and the Jeanne and J.-Louis Lévesque

Chair in Radiobiology. We wish to acknowledge the cyclotron team, Dr. Samia Ait-Mohand and the LabTEP laboratory staff at the CIMS for their assistance in the realization of this work.

REFERENCES

(1) Louie, A. (2010) Multimodality Imaging Probes: Design and Challenges. *Chem. Rev. 110*, 3146−3195.
(2) Yin Zhang, Y., Yang, Y., and Cai, W. (2011) Multimodality Imaging of Integrin $\alpha_v\beta_3$ Expression. *Theranostics 1*, 135−148.
(3) Liu, Y., Yu, G., Tian, M., and Zhang, H. (2011) Optical probes and the applications in multimodality imaging. *Contrast Media Mol. Imaging 6*, 169−177.
(4) Nesterova, I. V., Erdem, S. S., Pakhomov, S., Hammer, R. P., and Soper, S. A. (2009) Phthalocyanine dimerization-based molecular beacons using near-IR fluorescence. *J. Am. Chem. Soc. 25*, 2432−2433.
(5) Moan, J., Iani, V., and Ma, L., W. (1998) *In vivo* fluorescence of phthalocyanines during light exposure. *J. Photochem. Photobiol. B 42*, 100−103.
(6) Witjes, M. J. H., Speelman, O. C., Nikkels, P. G. J., Nooren, C. A. A. M., Nautal, J. M., van der Holt, B., van Leengoed, H. L. L. M., Star, W. M., and Roodenburg, J. L. N. (1996) *In vivo* fluorescence kinetics and localisation of aluminium phthalocyanine disulphonate in an autologous tumour model. *Br. J. Cancer 73*, 573−580.
(7) Peng, Q., Moan, J., Nesland, J. M., and Rimington, C. (1990) Aluminum phthalocyanines with asymetrical lower sulfonation and with symmetrical higher sulfonation: a comparison of localizing and photosensitizing mechanism in human tumor lox xenografts. *Int. J. Cancer 46*, 719−726.
(8) Rousseau, J., Ali, H., Lamoureux, G., LeBel, E., and van Lier, J. E. (1985) Synthesis, tissue distribution and tumor uptake of ^{99m}Tc- and ^{67}Ga-tetrasulfophthalocyanine. *Int. J. Appl. Radiat. Isot. 36*, 709−716.
(9) Chan, W. S., Marshall, J. F., and Hart, I. R. (1989) Effect of tumour location on selective uptake and retention of phthalocyanines. *Cancer Lett. 44*, 73−77.
(10) Chan, W. S., Marshall, J. F., Svensen, R., Bedwell, J., and Hart, I. R. (1990) Effect of sulfonation on the cell and tissue distribution of the photosensitizer aluminium phthalocyanine. *Cancer Res. 50*, 4533−4538.
(11) Ranyuk, E. R., Cauchon, N., Ali, H., Guérin, B., and van Lier, J. E. (2011) Synthesis and *in vivo* biodistribution studies of Cu-64 labeled sulfonated phthalocyanines for positron emission tomography. *Bioorg. Med. Chem. Lett. 21*, 7470−7473.
(12) Kolarova, H., Nevrelova, P., Bajgar, R., Jirova, D., Kejlova, K., and Strnad, M. (2007) *In vitro* photodynamic therapy on melanoma cell lines with phthalocyanine. *Toxicol. in Vitro 21*, 249−253.
(13) Cauchon, N., Tian, H., Langlois, R., La, M. C., Martin, S., Ali, H., Hunting, D., and van Lier, J. E. (2005) Structure-photodynamic activity relationships of substituted zinc trisulfophthalocyanines. *Bioconjugate Chem. 16*, 80−89.
(14) Kudrevich, S., Brasseur, N., La, M. C., Gilbert, S., and van Lier, J. E. (1997) Syntheses and photodynamic activities of novel trisulfonated zinc phthalocyanine derivatives. *J. Med. Chem. 40*, 3897−3904.
(15) Ward, A. J., and Matthews, E. K. (1996) Cytotoxic, nuclear, and growth inhibitory effects of photodynamic drugs on pancreatic carcinoma cells. *Cancer Lett. 102*, 39−47.
(16) Glassberg, E., Lewandowski, L., Lask, G., and Uitto, J. (1990) Laser-induced photodynamic therapy with aluminum phthalocyanine tetrasulfonate as the photosensitizer: differential phototoxicity in normal and malignant human cells *in vitro*. *J. Invest. Dermatol. 94*, 604−610.
(17) Paquette, B., Ali, H., Langlois, R., and van Lier, J. E. (1988) Biological activities of phthalocyanines-VIII. Cellular distribution in V-79 Chinese hamster cells and phototoxicity of selectively sulfonated aluminum phthalocyanines. *Photochem. Photobiol. 47*, 215−220.
(18) Chan, W. S., Brasseur, N., La, M. C., Ouellet, R., and van Lier, J. E. (1997) Efficacy and mechanism of aluminium phthalocyanine and its sulphonated derivatives mediated photodynamic therapy on murine tumours. *Eur. J. Cancer 33*, 1855−1859.
(19) Stylli, S. S., Hill, J., Sawyer, W., and Kaye, A. (1995) Aluminium phthalocyanine mediated photodynamic therapy in experimental malignant glioma. *J. Clin. Neurosci. 2*, 146−151.
(20) Stylli, S. S., Hill, J. S., Sawyer, W. H., and Kaye, A. H. (1995) Phthalocyanine photosensitizers for the treatment of brain tumours. *J. Clin. Neurosci. 2*, 64−72.
(21) Peng, Q., and Moan, J. (1995) Correlation of distribution of sulphonated aluminium phthalocyanines with their photodynamic effect in tumour and skin of mice bearing CaD2 mammary carcinoma. *Br. J. Cancer 72*, 565−574.
(22) Chan, W. S., West, C. M., Moore, J. V., and Hart, I. R. (1991) Photocytotoxic efficacy of sulphonated species of aluminium phthalocyanine against cell monolayers, multicellular spheroids and in vivo tumours. *Br. J. Cancer 64*, 827−832.
(23) Tralau, C. J., Macrobert, A. J., Coleridge-Smith, P. D., Barr, H., and Bown, S. G. (1987) Photodynamic therapy with phthalocyanine sensitisation: quantitative studies in a transplantable rat fibrosarcoma. *Br. J. Cancer 55*, 389−395.
(24) Sandeman, D. R., Bradford, R., Buxton, P., Bown, S. G., and Thomas, D. G. (1987) Selective necrosis of malignant gliomas in mice using photodynamic therapy. *Br. J. Cancer 55*, 647−649.
(25) Kessel, D. (1998) PDT: expanding the database, an update on new drugs and mechanisms of phototoxicity. *Int. Photodynamics 1*, 2−4.
(26) Sekkat, N., van den Bergh, H., Nyokong, T., and Lange, N. (2012) Like a Bolt from the Blue: Phthalocyanines in Biomedical Optics. *Molecules 17*, 98−144.
(27) Lebel, R., Zarifyussefian, N., Letendre-Jauniaux, M., Daigle, O., Ranyuk, E., Van Lier, J., Guérin, B., Lecomte, R., Massonneau, M., Ducharme, M.-E., and Bérubé Lauzière, Y.. Ultra-high sensitivity detection of bimodal probes at ultra-low noise for combined fluorescence and positron emission tomography imaging; *Proc. SPIE 8574*, Multimodal Biomedical Imaging VIII; SPIE BiOS - Photonics West, San Francisco, CA, U.S.A., 2013; pp 85740M 1−7.
(28) Clarke, E. T. M. (1992) Stabilities of trivalent metal ion complexes of the tetraacetate derivatives of 12-, 13-, and 14-membered tetraazamacrocycles. *Inorg. Chim. Acta 190*, 37−46.
(29) Wadas, T. W., Wong, E. H., Weisman, G. R., and Anderson, C. J. (2010) Coordinating Radiometals of Copper, Gallium, Indium, Yttrium and Zirconium for PET and SPECT Imaging of Disease. *Chem. Rev. 110*, 2858−2902.
(30) Fournier, P., Dumulon-Perreault, V., Ait-Mohand, S., Tremblay, S., Bénard, F., Lecomte, R., and Guérin, B. (2012) Novel radiolabeled peptides for breast and prostate tumor PET imaging: ^{64}Cu/ and ^{68}Ga/NOTA-PEG-[D-Tyr^6,βAla^{11},Thi^{13},Nle^{14}]BBN(6−14). *Bioconjugate Chem. 3*, 1687−1693.
(31) McCarthy, D. W., Shefer, R. E., Klinkowstein, R. E., Bass, L. A., Margeneau, W. H., Cutler, C. S., Anderson, C. J., and Welch, M. J. (1997) Efficient production of high specific activity ^{64}Cu using a biomedical cyclotron. *Nucl. Med. Biol. 24*, 35−43.
(32) Zhernosekov, K. P., Filosofov, D. V., Baum, R. P., Aschoff, P., Bihl, H., Razbash, A. A., Jahn, M., Jennewein, M., and Rosch, F. (2007) Processing of generator-produced ^{68}Ga for medical application. *J. Nucl. Med. 48*, 1741−1748.
(33) Li, M., and Dixon, D. J. (2010) Stereoselective Spirolactam Synthesis via Palladium Catalyzed Arylative Allene Carbocyclization Cascades. *Org. Lett. 12*, 3784−3787.
(34) Lu, B., Li, C., and Zhang, L. (2010) Gold-Catalyzed Highly Regioselective Oxidation of C−C Triple Bonds without Acid Additives: Propargyl Moieties as Masked α,β-Unsaturated Carbonyls. *J. Am. Chem. Soc. 132*, 14070−14072.
(35) Loening, A. M., and Gambhir, S. S. (2003) AMIDE: a free software tool for multimodality medical image analysis. *Mol. Imaging. 2*, 131−7.
(36) Tian, H., Ali, H., and van Lier, J. E. (2000) Synthesis of water soluble trisulfonated phthalocyanines via palladium-catalysed cross coupling reactions. *Tetrahedron Lett. 41*, 8435−8438.

(37) Tully, S. E., and Cravatt, B. F. (2010) Activity-Based Probes That Target Functional Subclasses of Phospholipases in Proteomes. *J. Am. Chem. Soc. 132*, 3264−3265.
(38) Murgu, I., Baumes, J. M., Eberhard, J., Gassensmith, J. J., Arunkumar, E., and Smith, B. D. (2010) Macrocycle Breathing in [2]Rotaxanes with Tetralactam Macrocycles. *J. Org. Chem. 75*, 6516−6531.
(39) Balraju, V., Reddy, D. S., Periasamy, M., and Igbal, J. (2005) Synthesis of conformationally constrained cyclic peptides using an intramolecular Sonogashira coupling. *J. Org. Chem. 70*, 9626−9628.
(40) Ranyuk, E., Cauchon, N., Klarskov, K., Guérin, B., and van Lier, J. E. (2013) Phthalocyanine-Peptide Conjugates: Receptor-Targeting Bifunctional Agents for Imaging and Photodynamic Therapy. *J. Med. Chem. 56*, 1520−1534.